NIH Public Access
Author Manuscript
Genesis. Author manuscript; available in PMC 2009 February 7.

Published in final edited form as:
Genesis. 2008 August ; 46(8): 431–439. doi:10.1002/dvg.20418.

Generation of a conditional mutant allele for *Tab1* in mouse

Maiko Inagaki[1], **Yoshihiro Komatsu**[2], **Greg Scott**[3], **Gen Yamada**[4], **Manas Ray**[3], **Jun Ninomiya-Tsuji**[1], and **Yuji Mishina**[2,3,*]

1*Department of Environmental and Molecular Toxicology, North Carolina State University, Raleigh, NC 27695-7633 USA*

2*Laboratory of Reproductive and Developmental Toxicology, NIEHS, National Institute of Health, Research Triangle Park, NC 27709, USA*

3*Knock Out Core, National Institute of Health, Research Triangle Park, NC 27709, USA*

4*Center for Animal Resources and Development, Graduate School of Molecular and Genomic Pharmacy, Kumamoto University, Kumamoto, 860-0811, JAPAN*

Abstract

TAK1 binding protein1 (TAB1) binds and induces autophosphrylation of TGF-β activating kinase (TAK1). TAK1, a mitogen activated kinase kinase kinase, is involving in several distinct signaling pathways including non-Smad pathways for TGF-β superfamily members and inflammatory responses caused by cytokines. Conventional disruption of the murine *Tab1* gene results in late gestation lethality showing intraventricular septum defects and under developed lung alveoli. To gain a better understanding of the roles of TAB1 in different tissues at different stages of development and in pathological conditions, we generated *Tab1* floxed mice in which loxP sites flank exons 9 and 10 to remove the C-terminal region of TAB1 protein necessary for activation of TAK1. We demonstrate that Cre-mediated recombination using *Sox2-Cre*, a Cre line expressed in the epiblast during early embryogenesis, results in deletion of the gene and protein. These homozygous Cre-recombined null embryos display an identical phenotype to conventional null embryos. This animal model will be useful to reveal distinct roles of TAB1 in different tissues at different stages.

Introduction

The transforming growth factor-beta (TGF-β) superfamily members including bone morphogenetic proteins (BMPs), growth and differentiation factors (GDFs), nodal /lefties, activins, and Mullerian inhibitory substance, exert a wide range of functions during early patterning of embryos, organogenesis, and physiological regulations after birth (de Caestecker, 2004; Kishigami and Mishina, 2005). Numerous reports indicate that Smad proteins are involving in the signaling pathway activated by members of the TGF-β superfamily (Miyazono *et al.*, 2005; Whitman, 1998). In addition to the canonical signaling pathway mediated by Smad proteins, it is shown that mitogen-activated protein (MAP) kinase pathways are involved in the TGF-β superfamily signaling pathways (Aubin *et al.*, 2004; Kretzschmar *et al.*, 1997). The MAP kinase pathway is a conserved eukaryotic signaling module regulated through a three-tiered kinase cascade composed of MAP kinase kinase kinase (MAPKKK), MAP kinase kinase (MAPKK), and MAP kinase (MAPK) (Johnson and Lapadat, 2002; Pearson *et al.*, 2001).

*Corresponding Author: Yuji Mishina Laboratory of Reproductive and Developmental Toxicology, NIEHS, National Institute of Health, Research Triangle Park, NC 27709 919-541-1095 919-541-3800 (fax) mishina@niehs.nih.gov

NIH-PA Author Manuscript
NIH-PA Author Manuscript
NIH-PA Author Manuscript

NIH-PA Author Manuscript

NIH-PA Author Manuscript

NIH-PA Author Manuscript

TGF-β Activation Kinase 1 (TAK1) was originally found as a MAPKKK of which activity is upregulated by TGF-β treatment (Yamaguchi *et al.*, 1995). TAK1 participates in the non-Smad pathway by activating p38 and SnoN degradation (Hanafusa *et al.*, 1999; Kajino *et al.*, 2007). Besides the TGF-β signaling pathway, TAK1 is involved in several innate immune signaling pathways including cytokines TNF and IL-1, Toll-like receptors and intracellular bacterial sensor NOD-like receptor NOD1/2 pathways (Hasegawa *et al.*, 2008; Kim *et al.*, 2008; Ninomiya-Tsuji *et al.*, 1999; Shim *et al.*, 2005; Takaesu *et al.*, 2003). The innate stimuli-activated TAK1 also induces activation of transcription factor AP-1 through MAPKs such as c-Jun N-terminal kinase (JNK) and p38. It has been reported that TAK1 is critically involved in stress-activated cell signaling (Chen *et al.*, 2002; Singhirunnusorn *et al.*, 2005) including osmotic stress-induced JNK activation (Huangfu *et al.*, 2006).

Using TAK1 protein as a bait, TAK1 binding protein 1 (TAB1, *Map3k7ip1*) (Shibuya *et al.*, 1996) and TAK1 binding protein 2/3 (TAB2/3) (Ishitani *et al.*, 2003; Takaesu *et al.*, 2000) are previously identified. TAB2 and its homolog TAB3 function as an adaptor tethering TAK1 to the IKK complex for ubiquitination (Kanayama *et al.*, 2004; Kishida *et al.*, 2005). In cultured cells, TAB1 is constitutively associated with endogenous TAK1 (Kishimoto *et al.*, 2000). TAB1 induces TAK1 autophosphorylation and thereby catalytically activates TAK1 kinase activity in vitro (Kishimoto *et al.*, 2000). Among a total of 502 amino acid residues of TAB1, only 16 residues in the C-terminal region (480-495 aa.) are essential for TAK1-TAB1 binding, and 68 residues (437-504 aa.) are sufficient for the autophosphorylation/activation of TAK1 following the binding (Ono *et al.*, 2001). It was demonstrated that the TAK1-TAB1 complex interacts with BMP receptors via X-linked inhibitor of apoptosis protein (IAP), supporting further the idea that TAK1-TAB1 is involved in mediating BMP signaling as a non-Smad pathway (Yamaguchi *et al.*, 1999).

TAB1 is encoded by 11 exons on chromosome 15 in mice. Previously, *Tab1*-deficient mice were generated by deleting exon 9 and 10 of *Tab1*, which encode the C-terminal region of TAB1 (308-434 aa.) (Komatsu *et al.*, 2002). An alternative splicing between exon 8 and 11, if present, causes flameshift and the aforementioned domain necessary for TAK1 binding and subsequent activation is not produced (Komatsu *et al.*, 2002; Ono *et al.*, 2001). Therefore, TAB1 protein without the C-terminus (TAB1ΔC), if present in the homozygous mutants, should be functionally inactive regarding TAK1-mediated signaling pathways. Homozygous mice for the *Tab1*-deficient allele were embryonic lethal with several developmental dysregulations including failure of cardiovascular morphogenesis (Komatsu *et al.*, 2002). Until mid gestation, *Tab1* mutant embryos develop without overt abnormalities, however, they start to show a bloated appearance as early as E15.5 and die at term (Komatsu *et al.*, 2002). Histological observation reveal that thinner ventricular wall and defects in intra ventricular septum formation in the heart as well as degeneration of terminal bud epithelium and failure of expansion of alveoli in the lung (Komatsu *et al.*, 2002). It is notable that *Id2* expression in the lung epithelium is downregulated in the mutant embryos and response to TGF-β treatment is impaired in the *Tab1* deficient mouse embryonic fibroblasts (MEFs) suggesting the involvement of TAB1 in TGF-β and BMP pathways (Komatsu *et al.*, 2002).

It is an interesting contrast that *Tak1* conventional knockout embryos are lethal by E9.5 (Jadrich *et al.*, 2006; Sato *et al.*, 2005; Shim *et al.*, 2005), whereas *Tab1* knockout embryos are grossly normal by embryonic day 14.5 (E14.5) (Komatsu *et al.*, 2002). These facts prompted us to speculate that TAB1 is essential for some, but not all, of the TAK1-mediated signaling pathways. Indeed, studies using TAB1 deficient MEFs reported that TNF-, and IL-1-induced activation of NF-κB, JNK and p38 are intact in TAB1-deficient MEFs (Shim *et al.*, 2005).

Cell type-specific gene ablation by *Cre-loxP* technology is particularly useful for determining the distinct tissue-specific function of a gene that is lethal when deleted (Kwan, 2002). To

NIH-PA Author Manuscript

NIH-PA Author Manuscript

NIH-PA Author Manuscript

overcome the perinatal lethality occurring with the conventional deletion of the *Tab1* locus, and elucidate further the functions of TAB1 in BMP signaling pathways and other cytokine signaling pathways in adult mice, we generated a conditional allele of *Tab1* using Cre-loxP technology.

Results and Discussion

Generation of a universal vector for conditional gene targeting

To facilitate vector construction for gene targeting to generate a conditional allele, first we prepared a vector which allows for directional cloning of PCR amplified genomic fragments. A *Pgk-neo* selection cassette was flanked by FRT sites (Dymecki, 1996) and two loxP sites were placed outside of the *FRT-Pgk-neo-FRT* cassette. A MC-DTA cassette (Yagi *et al.*, 1993) was also included for negative selection. Multicloning sites for a series of rare-cutting enzymes were added in 3 places; between the DTA cassette and one of the loxP site, the FRT-Pgk-neo-FRT cassette and the other loxP site, and the other loxP site and the vector backbone (Fig. 1). These multicloning sites allow introducing genomic PCR products amplified with primers having corresponding enzyme recognition sequences at the ends of each primer. Each multicloning site has at least 2 cut sites that allow directional cloning, if applicable. Furthermore, we added three more rare cutter sites for linearizing targeting vectors prior to electroporation to ES cells. We named this all-in-one type vector the Multiple Amplicon Insertion Knock Out (MAIKO) vector.

Generation of the conditional allele of Tab1

Our targeting vector was designed to introduce one *lox*P site and an *FRT-Pgkneo-FRT* cassette to intron 8 and the other *lox*P to intron 10 (Fig. 1 and 2). By this way, exon 9 and 10, the same exons we previously deleted by a conventional gene knockout method, were flanked by the *lox*P sites. *Cre*-dependent DNA recombination results in the deletion of the C-terminus of the TAB1 protein essential for TAK1 binding and subsequent activation (Ono *et al.*, 2001). Therefore, the protein product from the Cre-recombined allele, if present, should be functionally inactive regarding TAK1-mediated signaling pathways. After positive and negative selection with G418 and DT-A, correctly targeted ES cell clones were screened by Southern blot analysis (Fig. 2). Targeted ES clones were injected into blastocysts for germline transmission. Note that we used FRT sites to flank the neo cassette for an option to remove the neo gene with Flp recombinase.

Confirmation of deletion of Tab1 allele using Cre-loxP approach

Correct targeting events were confirmed by Southern blotting using 5′ and 3′ external probes, and the presence of the 5′ *loxP* site was confirmed by the 3′ external probe for the presence of an 8 kb band with *Eco*RI digestion (Fig. 2A,B). The targeted allele was designated as the *floxP +neo* (*fn*) allele. After confirmation of germline transmission, F1 offspring heterozygous for *fn* were intercrossed to generate mice homozygous for *fn*. The resulting F2 showed the expected ratio (+/+:*fn*/+:*fn*/*fn* = 22:55:20, 12 litters) of offspring. In addition, F1 offspring heterozygous for *fn* were bred with *ROSA26-Flp* mice, containing FLP recombinase, to remove the neo cassette through recombination at the FRT site. Removal of the neo was confirmed by PCR (Fig. 3). The targeted allele without the neo cassette was designated *floxP* (*fx*) allele. Intercrosses between mice heterozygous for the *fx* allele generated the expected ratio of the mice homozygous for *fx* (+/+:*fx*/+:*fx*/*fx* = 10:20:12). To verify whether the loxP sites are functional, mice heterozygous for *fn* were bred with *Sox2-Cre* transgenic mice, producing Cre in the epiblast cells, to remove the floxed exon 9 and 10. Offspring were analyzed by PCR confirmation of Cre-dependent deletion as well as the efficiency of Cre recombination of the floxed allele *in vivo* (Fig. 3). The Cre-recombined allele was designated as *ΔE* allele.

NIH-PA Author Manuscript

NIH-PA Author Manuscript

NIH-PA Author Manuscript

Next we examined the functionality of the conditional (*fn* and *fx*) alleles by generating heterozygous mice for *fn* or *fx* allele over the Cre-recombined allele. Breeding between heterozygous mice for the Cre-recombined allele (*ΔE*/+) and the allele homozygous for *fx* (*fx*/*fx*) resulted in an expected ratio of pups at the weaning age (*fx*/+:*fx*/*ΔE* = 19:25, 6 litters). However, we failed to get *fn*/*ΔE* mice at weaning stage from the breeding between heterozygous mice for Cre-recombined allele (*ΔE*/+) and homozygous allele for *fn* (*fn*/*fn*) (*fn*/+:*fn*/*ΔE* = 18:0, 4 litters). These results suggest that the presence of the neo cassette in the *Tab1* locus makes the gene hypomorphic. Indeed, expression levels of TAB1 from the *fn* allele is much lower than that from the wild-type allele and the *fx* allele in keratinocytes isolated from newborn skin (supplemental figure 1). Phenotypic analyses of the *fn*/*ΔE* embryos would be informative if they showed less severe phenotypes than these found in previously reported conventional knockout embryos and homozygous mice for Cre-recombined allele (see below).

Similarities of embryonic phenotype in both the conventional Tab1 null and the Cre-recombined Tab1 mice

Mice that were heterozygous for the Cre-recombined allele were intercrossed to obtain mice homozygous for Cre-recombined *Tab1* allele (*ΔE*/*ΔE*). The phenotype obtained from this cross was compared to that in the conventional *Tab1* null mice previously reported (Komatsu *et al.*, 2002).

As is evident in Fig. 4, homozygous mice for the Cre-recombined allele developed similar developmental morphological abnormalities at E16.5 similar to abnormalities of conventional *Tab1* null embryos, including edema and hemorrhage (Fig.4 A, B). Western blot using an antibody against C-terminal region of TAB1 failed to detect presence of TAB1 in extracts from *ΔE*/*ΔE* embryos (Fig. 4C). Histological examination revealed that embryos homozygous for the Cre recombined allele developed similar intraventricular septum defects (VSD) (Fig. 4D-F) and failure of expansion of alveoli in the lung (Fig. 4G-L) found in embryos homozygous for conventionally targeted allele.

It has been reported that TAB1 is involved in BMP signaling for mesoderm induction in *Xenopus* (Shibuya *et al.*, 1998) and epithelial-mesenchymal interaction of lung morphogenesis in mouse embryos (Komatsu *et al.*, 2002). To further elucidate the involvement of TAB1 in BMP signaling pathways, we examined the expression pattern of *Id1* in intestine. Id genes are putative targets of BMP signals (Hollnagel *et al.*, 1999). It is reported that *Bmp2* and *Bmp4* are expressed in intestinal mesenchyme (Karlsson *et al.*, 2000). Especially, *Id1* is known as a target gene of BMP4 expressing in mesenchymal tissues of intestine. Thus, we hypothesized that *Id1* gene function may be aberrant in the intestinal mesenchyme of *Tab1* mutant embryos. As expected, expression of *Id1* in mesenchymal components of intestine was severely reduced in the *Tab1* conventional null embryos at E16.5 (Fig. 5A). In addition, *Id1* expression level was upregulated by treatment of control MEF cells with BMP4 at 10 ng/ml and 20 ng/ml (Fig. 5B and data not shown), whereas expression of *Id1* was not changed when conventional *Tab1* null MEFs were treated with BMP4 (Fig. 5B). These results suggest that TAB1/TAK1 is involving in BMP signaling pathways to regulate downstream target genes such as *Id1*.

It is a formal possibility that a transcript from exon 1 to exon 8 is present and the N-terminal region of TAB1 encoded by these exons is produced. Indeed, we were able to detect such transcripts by RT-PCR in embryos homozygous for the Cre-recombined allele as well as in embryos homozygous for the conventionally targeted allele (supplemental figure 2 and data not shown, respectively). Unfortunately, the only TAB1 antibody available recognizes the C-terminal region and not the N-terminus of TAB1. However, as mentioned above, domains necessary for TAK1 binding and subsequent activation are located in the C-terminus of TAB1 (Ono *et al.*, 2001) encoded by exon 11, and removal of exon 9 and 10 by Cre-dependent recombination causes a frame shift that prevents expression of a functional C-terminal domain

NIH-PA Author Manuscript

NIH-PA Author Manuscript

NIH-PA Author Manuscript

(Fig. 4C). Therefore, it is likely that the floxed mouse line present here can be applied to inactive TAK1-mediated signaling pathways in a tissue-specific manner.

In conclusion, we have generated a conditional *Tab1* allele and shown that homozygous general deletion of exon 9 and 10 most likely leads to absence of C-terminal region of the TAB1 protein that is essential for binding to TAK1 for its activation, accompanied by embryonic lethality exemplified as VSD. In the future, crossing this floxed line with transgenic mice that express Cre-recombinase in a tissue-specific manner will facilitate studies determining the distinct roles of TAB1 in different tissues where it is normally expressed, and allow determination of relative importance in different signaling pathways mediated by TAK1.

MATERIALS AND METHODS

Generation of a *Tab1*-floxed allele

A 3.6-kb fragment containing exon 8 was PCR amplified from 129SvEv genomic DNA with Phusion polymerase (New England Biolabs, Inc. MA) using the following primers; 5′-GTGgcgatcgcCTACAGTGGCAGGGTTACCATGGA-3′ and 5′-GTGgcggccgcGCTGTTCAGatCtATCCTTCTGGAACGCACTGA-3′. *ASiS*I and *Not*I sites are shown in lower case. A 1.7-kb fragment containing exon 9 and 10 was also PCR amplified using the following primers; 5′- GCGttaattaaCTCAGGTTGCAATTGACTGGCAGA-3′ and 5′-CTCatcgatGAATTCCCACCTTGCCCTGAATCTCCACTT-3′. *Pac*I and *Cla*I sites are shown in lower case. A 5.8-kb fragment containing exon 11 was PCR amplified using the following primers; 5′-GTGggccggccCTTTCATCCATGGGCAGCTTCTCT-3′ and 5′-GTGggcgcgccGAGAGGTTGGCTCTAGTTTGTGCT-3′. *Fse*I and *Asc*I sites are shown in lower case. After amplification, these fragments were digested with restriction enzymes and ligated into the corresponding sites in the MAIKO vector (Fig. 1). The positions of the probes used for Southern analysis are shown in Fig. 2A. The sizes of the restriction fragments detected by these probes in WT and targeted DNA are shown above or below the locus. A 3′ *loxP* site is marked with an *Eco*RI site.

Linearized targeting vector was electroporated into 1.0×10^7 AB2.2 ES cells (Lexicon Genetics) and 1.6×10^7 clone A3 of UG347 ES cells, which we recently established from 129SvEv blastocysts. Three hundred G418-resistant ES cell clones from each cell line, a total of 600 clones, were initially screened by Southern blot and 33 correctly targeted ES cell clones were identified. Twenty-four of them were confirmed to possess the loxP site in intron 10 (*fn*/+). The ratio of these two types of clones obtained without or with the loxP site is close to 1:3 presumably is because the *loxP* site in intron 10 divides the right homologous arm in about a 1:3 ratio (Cheah *et al.*, 2000). The targeted ES clones were injected into blastocysts from C57BL/6 albino mice. The resulting chimeras were bred to C57BL/6 females and F1 agouti offspring were genotyped by Southern analyses. Five targeted clones were used for injection and two of them underwent germline transmission.

Subsequently, mice heterozygous for *Tab1* floxed allele with a *Pgk-neo* cassette (*fn*/+) were bred with Flipper mice (Farley *et al.*, 2000) to remove the neo cassette (*fx*/+). The *fn*/+ mice also were bred with Sox2-Cre mice (Hayashi *et al.*, 2002) to delete exon 9 and 10 to generate a recombined null allele (*ΔE*/+).

All animal experiments were conducted according to the U.S. Public Health Service policy on the humane care and use of animals. All animal procedures used in this study were approved by the National Institute of Environmental Health Sciences Institutional Animal Care and Use Committee.

NIH-PA Author Manuscript

NIH-PA Author Manuscript

NIH-PA Author Manuscript

Genotype analyses

Genotypes were determined by Southern blot with 5′ and 3′ external probes as shown in Fig. 2A. For PCR analyses (Fig. 3), primers A and B were used to amplify fragments from wildtype (232 bp) and the *Tab1* floxed alleles (267 bp for both *fn* and *fx*). Primers C and D were also used to amplify fragments from wildtype (209 bp) and *Tab1* floxed allele after removal of the neo cassette (588 bp, *fx*). Primers B and C were used to detect Cre-dependent deletion of the floxed region (384 bp for *ΔE*). Primers; A (5′-CCAATTCTCCACCCTCACCTT-3′), B (5′-CTACAGATGCATGAAGCCAGT-3′), C (5′-GTAACCTTGTACCCGTGAGTT-3′), D (5′-GCTGTGTAGGAGACTTAGAGA-3′).

In situ hybridization, Western blot, MEF culture, isolation of keratinocytes

Section *in situ* hybridization was performed by using standard procedures (Komatsu *et al.*, 2002) with a digoxigenin-labeled RNA probes for *Id1* (kindly provided by Dr. Hal Weintraub). *Tab1* MEF cells were established from E15.5 homozygous *Tab1* mouse embryos. *Tab1* MEF cells were grown in Dulbecco's modified Eagle's medium (DMEM) with 10 % fetal bovine serum. Keratinocytes derived from the skin of newborn mice were cultured in Eagle's minimal essential medium supplemented with 4% Chelex-treated bovine growth serum, 10 ug/mL human epidermal growth factor (Invitrogen), and 0.05 mM calcium chloride (Omori et al., JBC). Recombinant human BMP4 was purchased from R&D. Whole protein lysates was extracted from E16.5 embryos and subjected to Western blot using polyclonal antibodies against TAK1 and TAB1 described previously (Ninomiya-Tsuji *et al.*, 1999).

Reverse-transcription PCR

Total RNA was prepared from MEFs using the RNeasy protect mini-kit (Qiagen). cDNA was synthesized using TaqMan reverse transcription reagents (Applied Biosystems). PCR analysis was performed using the following primers: *Tab1* N-terminus specific primers, 5′-CCACTCTGTCACCTCTCTGGA-3′ (located in exon 2) and 5′-CAGTGTGCTCAGTGTTGAGCT-3′ (located in exon 3), which produce a 232 bp fragment; *Tab1* C-terminus specific primers, 5′-GGCTGTGGTAGACCGTGTAAA-3′ and 5′-GTGCTCTGGGCACTTGAGTAG-3′ (both located in exon 9), which produce a 210 bp fragment.

Supplementary Material

Refer to Web version on PubMed Central for supplementary material.

ACKNOWLEDGEMENTS

This work was supported by the Intramural Research Program of the NIEHS, NIH to Y. M. and by a grant from NIH to J. N-T. Y. K. is supported, in part, by a fellowship from the Japan Society for the Promotion of Science.

REFERENCES

Aubin J, Davy A, Soriano P. In vivo convergence of BMP and MAPK signaling pathways: impact of differential Smad1 phosphorylation on development and homeostasis. Genes Dev 2004;18:1482–1494. [PubMed: 15198985]

Cheah SS, Kwan KM, Behringer RR. Requirement of LIM domains for LIM1 function in mouse head development. Genesis 2000;27:12–21. [PubMed: 10862151]

Chen W, White MA, Cobb MH. Stimulus-specific requirements for MAP3 kinases in activating the JNK pathway. J Biol Chem 2002;277:49105–49110. [PubMed: 12351623]

de Caestecker M. The transforming growth factor-beta superfamily of receptors. Cytokine Growth Factor Rev 2004;15:1–11. [PubMed: 14746809]

NIH-PA Author Manuscript

NIH-PA Author Manuscript

NIH-PA Author Manuscript

Dymecki SM. A modular set of Flp, FRT and lacZ fusion vectors for manipulating genes by site-specific recombination. Gene 1996;171:197–201. [PubMed: 8666272]

Farley FW, Soriano P, Steffen LS, Dymecki SM. Widespread recombinase expression using FLPeR (flipper) mice. Genesis 2000;28:106–110. [PubMed: 11105051]

Hanafusa H, Ninomiya-Tsuji J, Masuyama N, Nishita M, Fujisawa J, Shibuya H, Matsumoto K, Nishida E. Involvement of the p38 mitogen-activated protein kinase pathway in transforming growth factor-beta-induced gene expression. J Biol Chem 1999;274:27161–27167. [PubMed: 10480932]

Hasegawa M, Fujimoto Y, Lucas PC, Nakano H, Fukase K, Nunez G, Inohara N. A critical role of RICK/RIP2 polyubiquitination in Nod-induced NF-kappaB activation. Embo J 2008;27:373–383. [PubMed: 18079694]

Hayashi S, Lewis P, Pevny L, McMahon AP. Efficient gene modulation in mouse epiblast using a Sox2Cre transgenic mouse strain. Gene Expr Patterns 2002;2:93–97. [PubMed: 12617844]

Hollnagel A, Oehlmann V, Heymer J, Rüther U, Nordheim A. Id genes are direct targets of bone morphogenetic protein induction in embryonic stem cells. J Biol Chem 1999;274:19838–19845. [PubMed: 10391928]

Huangfu WC, Omori E, Akira S, Matsumoto K, Ninomiya-Tsuji J. Osmotic stress activates the TAK1-JNK pathway while blocking TAK1-mediated NF-kappaB activation: TAO2 regulates TAK1 pathways. J Biol Chem 2006;281:28802–28810. [PubMed: 16893890]

Ishitani T, Takaesu G, Ninomiya-Tsuji J, Shibuya H, Gaynor RB, Matsumoto K. Role of the TAB2-related protein TAB3 in IL-1 and TNF signaling. Embo J 2003;22:6277–6288. [PubMed: 14633987]

Jadrich JL, O'Connor MB, Coucouvanis E. The TGF beta activated kinase TAK1 regulates vascular development in vivo. Development 2006;133:1529–1541. [PubMed: 16556914]

Johnson GL, Lapadat R. Mitogen-activated protein kinase pathways mediated by ERK, JNK, and p38 protein kinases. Science 2002;298:1911–1912. [PubMed: 12471242]

Kajino T, Omori E, Ishii S, Matsumoto K, Ninomiya-Tsuji J. TAK1 MAPK kinase kinase mediates transforming growth factor-beta signaling by targeting SnoN oncoprotein for degradation. J Biol Chem 2007;282:9475–9481. [PubMed: 17276978]

Kanayama A, Seth RB, Sun L, Ea CK, Hong M, Shaito A, Chiu YH, Deng L, Chen ZJ. TAB2 and TAB3 activate the NF-kappaB pathway through binding to polyubiquitin chains. Mol Cell 2004;15:535–548. [PubMed: 15327770]

Karlsson L, Lindahl P, Heath J, Betsholtz C. Abnormal gastrointestinal development in PDGF-A and PDGFR-(alpha) deficient mice implicates a novel mesenchymal structure with putative instructive properties in villus morphogenesis. Development 2000;127:3457–3466. [PubMed: 10903171]

Kim JY, Omori E, Matsumoto K, Nunez G, Ninomiya-Tsuji J. TAK1 is a central mediator of NOD2 signaling in epidermal cells. J Biol Chem 2008;283:137–144. [PubMed: 17965022]

Kishida S, Sanjo H, Akira S, Matsumoto K, Ninomiya-Tsuji J. TAK1-binding protein 2 facilitates ubiquitination of TRAF6 and assembly of TRAF6 with IKK in the IL-1 signaling pathway. Genes Cells 2005;10:447–454. [PubMed: 15836773]

Kishigami S, Mishina Y. BMP signaling and early embryonic patterning. Cytokine Growth Factor Rev 2005;16:265–278. [PubMed: 15871922]

Kishimoto K, Matsumoto K, Ninomiya-Tsuji J. TAK1 mitogen-activated protein kinase kinase kinase is activated by autophosphorylation within its activation loop. J Biol Chem 2000;275:7359–7364. [PubMed: 10702308]

Komatsu Y, Shibuya H, Takeda N, Ninomiya-Tsuji J, Yasui T, Miyado K, Sekimoto T, Ueno N, Matsumoto K, Yamada G. Targeted disruption of the Tab1 gene causes embryonic lethality and defects in cardiovascular and lung morphogenesis. Mech Dev 2002;119:239–249. [PubMed: 12464436]

Kretzschmar M, Doody J, Massague J. Opposing BMP and EGF signalling pathways converge on the TGF-beta family mediator Smad1. Nature 1997;389:618–622. [PubMed: 9335504]

Kwan KM. Conditional alleles in mice: practical considerations for tissue-specific knockouts. Genesis 2002;32:49–62. [PubMed: 11857777]

Miyazono K, Maeda S, Imamura T. BMP receptor signaling: transcriptional targets, regulation of signals, and signaling cross-talk. Cytokine Growth Factor Rev 2005;16:251–263. [PubMed: 15871923]

NIH-PA Author Manuscript

NIH-PA Author Manuscript

NIH-PA Author Manuscript

Ninomiya-Tsuji J, Kishimoto K, Hiyama A, Inoue J, Cao Z, Matsumoto K. The kinase TAK1 can activate the NIK-I kappaB as well as the MAP kinase cascade in the IL-1 signalling pathway. Nature 1999;398:252–256. [PubMed: 10094049]

Ono K, Ohtomo T, Sato S, Sugamata Y, Suzuki M, Hisamoto N, Ninomiya-Tsuji J, Tsuchiya M, Matsumoto K. An evolutionarily conserved motif in the TAB1 C-terminal region is necessary for interaction with and activation of TAK1 MAPKKK. J Biol Chem 2001;276:24396–24400. [PubMed: 11323434]

Pearson G, Robinson F, Beers Gibson T, Xu BE, Karandikar M, Berman K, Cobb MH. Mitogen-activated protein (MAP) kinase pathways: regulation and physiological functions. Endocr Rev 2001;22:153–183. [PubMed: 11294822]

Sato S, Sanjo H, Takeda K, Ninomiya-Tsuji J, Yamamoto M, Kawai T, Matsumoto K, Takeuchi O, Akira S. Essential function for the kinase TAK1 in innate and adaptive immune responses. Nat Immunol 2005;6:1087–1095. [PubMed: 16186825]

Shibuya H, Iwata H, Masuyama N, Gotoh Y, Yamaguchi K, Irie K, Matsumoto K, Nishida E, Ueno N. Role of TAK1 and TAB1 in BMP signaling in early Xenopus development. Embo J 1998;17:1019–1028. [PubMed: 9463380]

Shibuya H, Yamaguchi K, Shirakabe K, Tonegawa A, Gotoh Y, Ueno N, Irie K, Nishida E, Matsumoto K. TAB1: an activator of the TAK1 MAPKKK in TGF-beta signal transduction. Science 1996;272:1179–1182. [PubMed: 8638164]

Shim JH, Xiao C, Paschal AE, Bailey ST, Rao P, Hayden MS, Lee KY, Bussey C, Steckel M, Tanaka N, Yamada G, Akira S, Matsumoto K, Ghosh S. TAK1, but not TAB1 or TAB2, plays an essential role in multiple signaling pathways in vivo. Genes Dev 2005;19:2668–2681. [PubMed: 16260493]

Singhirunnusorn P, Suzuki S, Kawasaki N, Saiki I, Sakurai H. Critical roles of threonine 187 phosphorylation in cellular stress-induced rapid and transient activation of transforming growth factor-beta-activated kinase 1 (TAK1) in a signaling complex containing TAK1-binding protein TAB1 and TAB2. J Biol Chem 2005;280:7359–7368. [PubMed: 15590691]

Takaesu G, Kishida S, Hiyama A, Yamaguchi K, Shibuya H, Irie K, Ninomiya-Tsuji J, Matsumoto K. TAB2, a novel adaptor protein, mediates activation of TAK1 MAPKKK by linking TAK1 to TRAF6 in the IL-1 signal transduction pathway. Mol Cell 2000;5:649–658. [PubMed: 10882101]

Takaesu G, Surabhi RM, Park KJ, Ninomiya-Tsuji J, Matsumoto K, Gaynor RB. TAK1 is critical for IkappaB kinase-mediated activation of the NF-kappaB pathway. J Mol Biol 2003;326:105–115. [PubMed: 12547194]

Whitman M. Smads and early developmental signaling by the TGFbeta superfamily. Genes Dev 1998;12:2445–2462. [PubMed: 9716398]

Yagi T, Nada S, Watanabe N, Tamemoto H, Kohmura N, Ikawa Y, Aizawa S. A novel negative selection for homologous recombinants using diphtheria toxin A fragment gene. Anal Biochem 1993;214:77–86. [PubMed: 8250258]

Yamaguchi K, Nagai S, Ninomiya-Tsuji J, Nishita M, Tamai K, Irie K, Ueno N, Nishida E, Shibuya H, Matsumoto K. XIAP, a cellular member of the inhibitor of apoptosis protein family, links the receptors to TAB1-TAK1 in the BMP signaling pathway. Embo J 1999;18:179–187. [PubMed: 9878061]

Yamaguchi K, Shirakabe K, Shibuya H, Irie K, Oishi I, Ueno N, Taniguchi T, Nishida E, Matsumoto K. Identification of a member of the MAPKKK family as a potential mediator of TGF-beta signal transduction. Science 1995;270:2008–2011. [PubMed: 8533096]

NIH-PA Author Manuscript

NIH-PA Author Manuscript

NIH-PA Author Manuscript

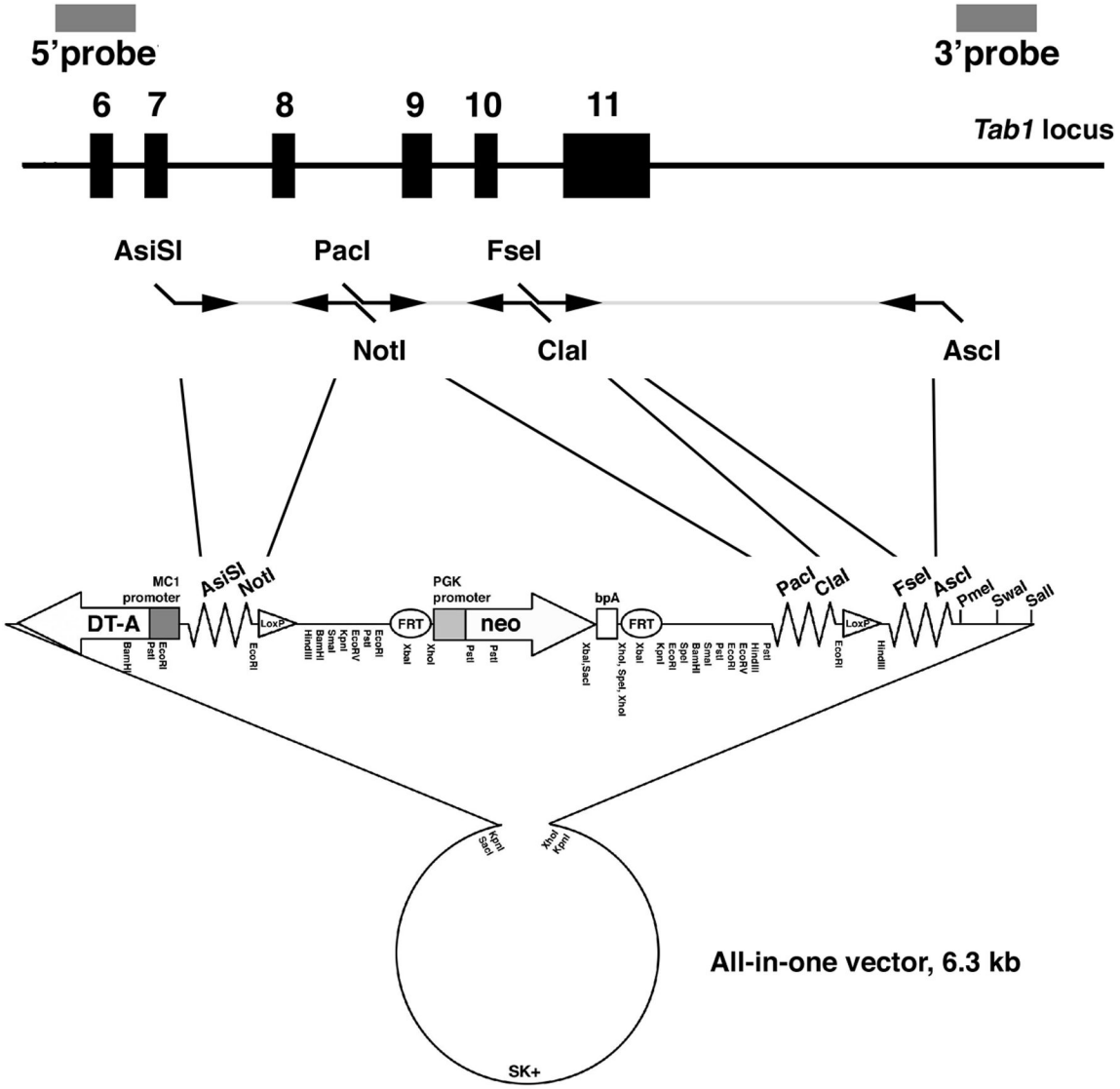

Figure 1. Structure of the all-in-one type Multiple Amplicon Insertion Knock Out (MAIKO) vector

A *Pgk-neo* cassette flanked by FRT sites for positive selection, a MC1-DTA cassette for negative selection, two loxP sites were produced with 3 rare cutter multicloning sites with. These configurations allow directional cloning of PCR amplified genomic fragments for both homologous arms and a floxed region. Bold indicates unique enzyme sites. For this study, genomic DNA was PCR amplified with primers designed to produce the enzyme sites indicated, and inserted into multicloning sites as shown.

NIH-PA Author Manuscript

NIH-PA Author Manuscript

NIH-PA Author Manuscript

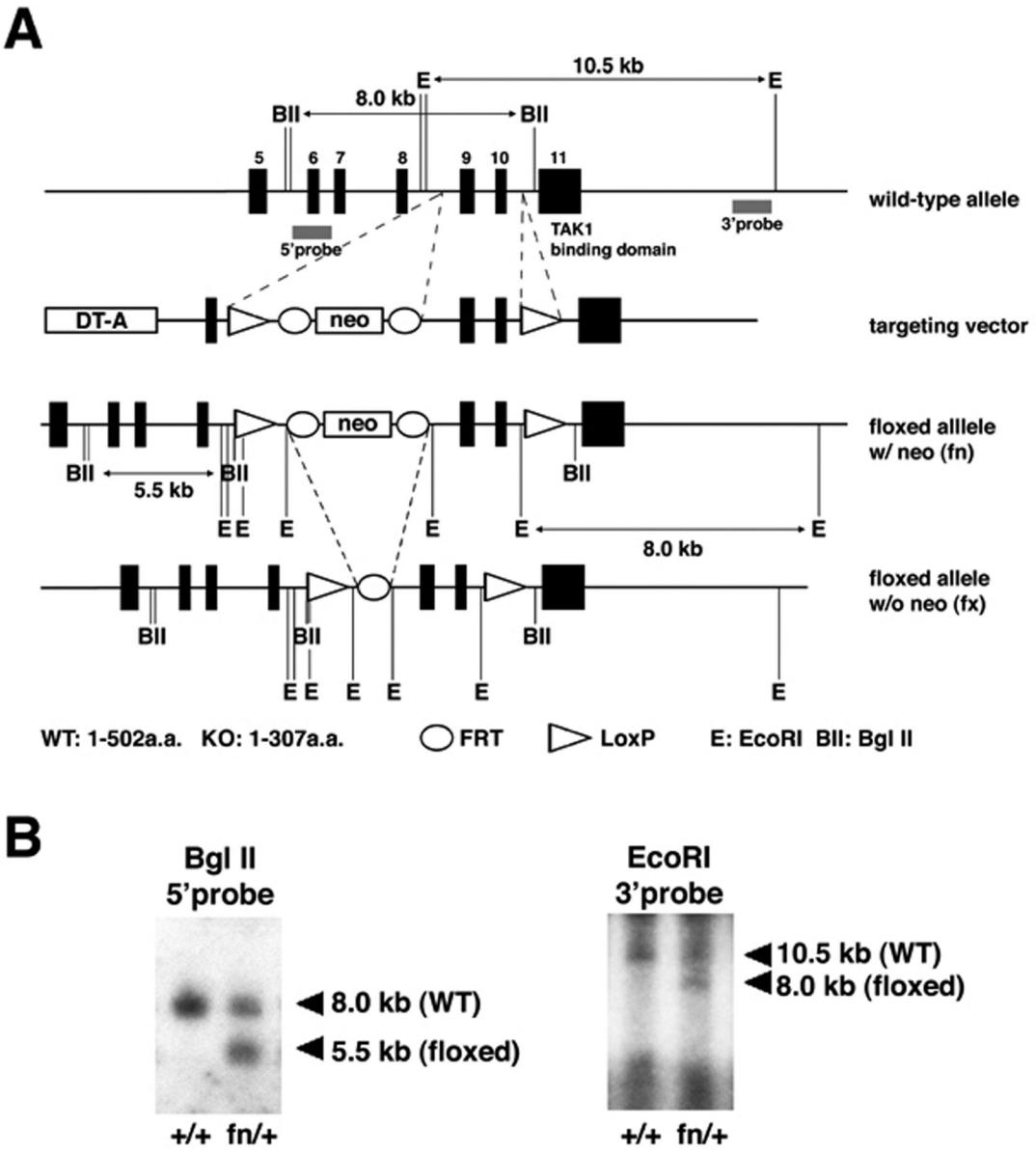

Figure 2. Targeted recombination of ES cells for *Tab1* locus

A. Genomic structure of *Tab1* locus and the targeting construct. A loxP site followed by *Pgk-neo* cassette flanked by FRT sites was inserted into intron 8. Another loxP site with an *Eco*RI site was inserted into intron 10. Positions of 5′ and 3′ external probes for Southern analyses and the sizes of the restriction fragments detected by these probes are shown. BII, *Bgl*II; E, *Eco*RI.

B. Confirmation of the targeting event in ES cells. Genomic DNA from WT ES cells (left lane, +/+) and correctly targeted cells (right lane, *fn*/+) were digested with enzymes and blots were hybridized with probes as indicated. *Eco*RI digestion and use of the 3′ probe confirmed the presence of the *lox*P site in intron 10.

NIH-PA Author Manuscript

NIH-PA Author Manuscript

NIH-PA Author Manuscript

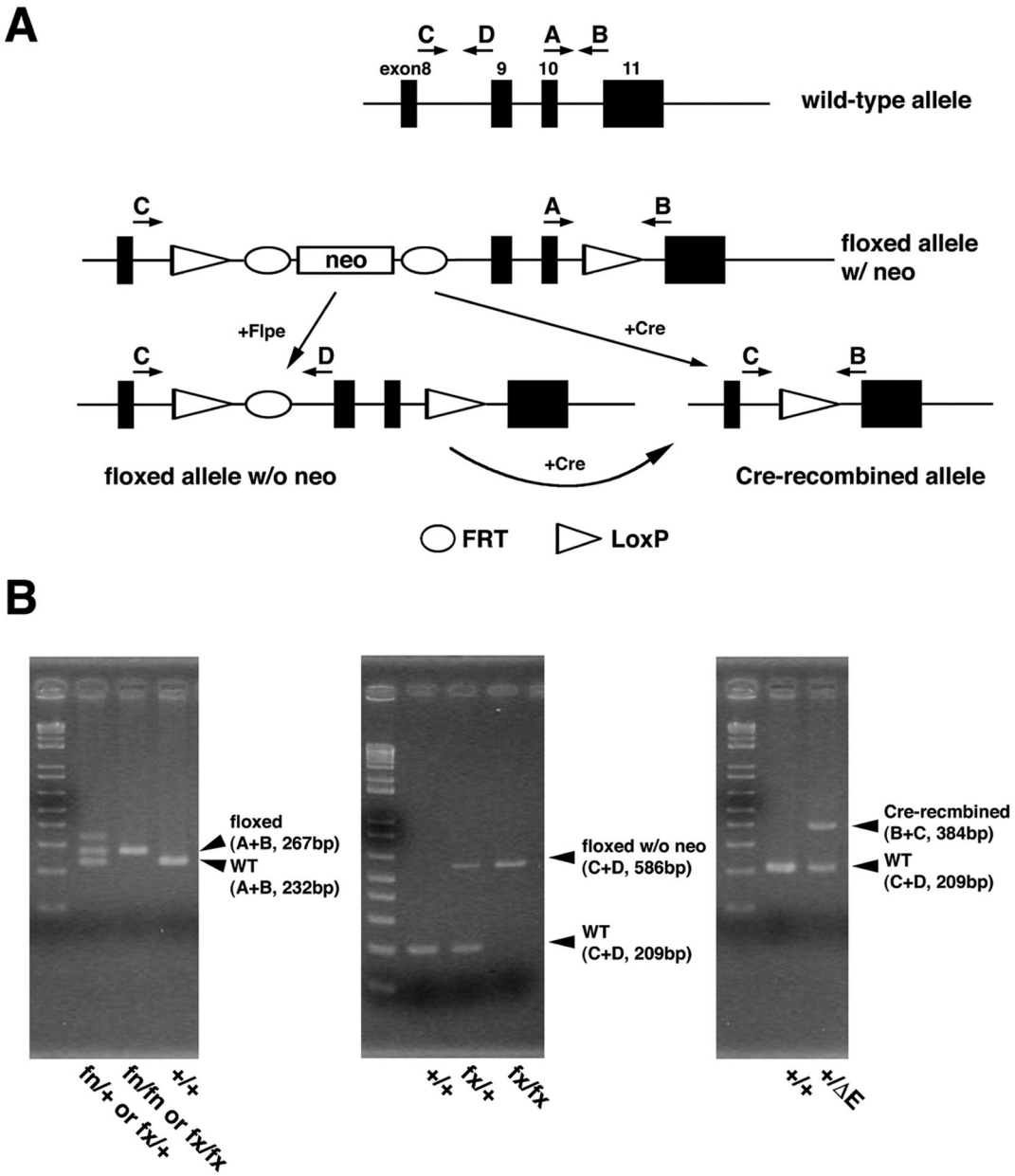

Figure 3. PCR strategy and genotyping

A. Schematic representation of structure of each allele and positions of primers. Primers A and B are used to differentiate the conditional allele from WT, whereas primers C and D are used to differentiate the *fx* allele from *fn*. Primers B and C are used to identify the Cre-recombined allele.

B. Genotyping results of the conditional allele. Combinations of the primers and sizes of the amplicons are indicated.

NIH-PA Author Manuscript
NIH-PA Author Manuscript
NIH-PA Author Manuscript

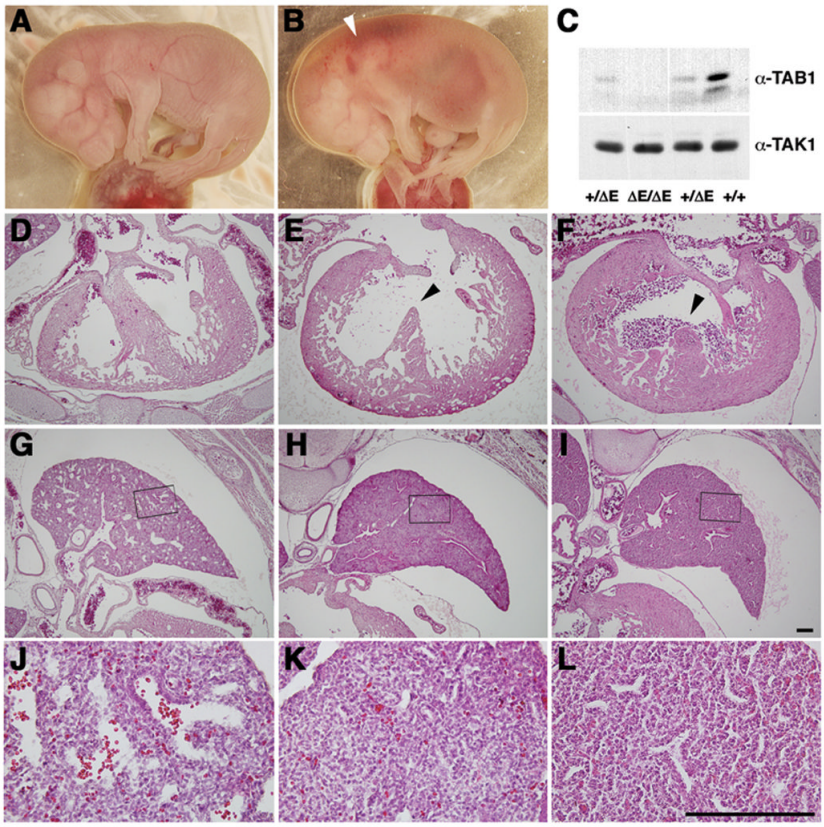

Figure 4. Homozygous embryos for Cre-recombined *Tab1* allele show similar developmental abnormalities to those of conventional knockout embryos

A-B. Whole view of embryos Wild-type (WT) and homozygous for Cre-recombined *Tab1* embryos (*ΔE/ΔE*) at E16.5. *Tab1 ΔE/ΔE* embryo shows edema and hemorrhage (white arrowhead).

C. Brain extracts from E16.5 embryos were subjected to western blotting using an anti-TAB1 antibody that recognizes the C-terminus of TAB1. TAK1 is shown as a loading control.

D-L. H&E staining of heart (D-F) and lung (G-L) sections from WT embryos (D, G, J), *Tab1 ΔE/ΔE* embryos (E, H, K), and conventional *Tab1*-deficient homozygous embryos (−/−) (F, I, L) at E16.5. J-K are higher magnification of G-I (boxed areas). *Tab1 ΔE/ΔE* embryo shows ventricular septum defects (arrowheads) and under expanded lung alveoli that are similar to these found in −/− embryos. Scale bar (D-L) = 200μm.

NIH-PA Author Manuscript

NIH-PA Author Manuscript

NIH-PA Author Manuscript

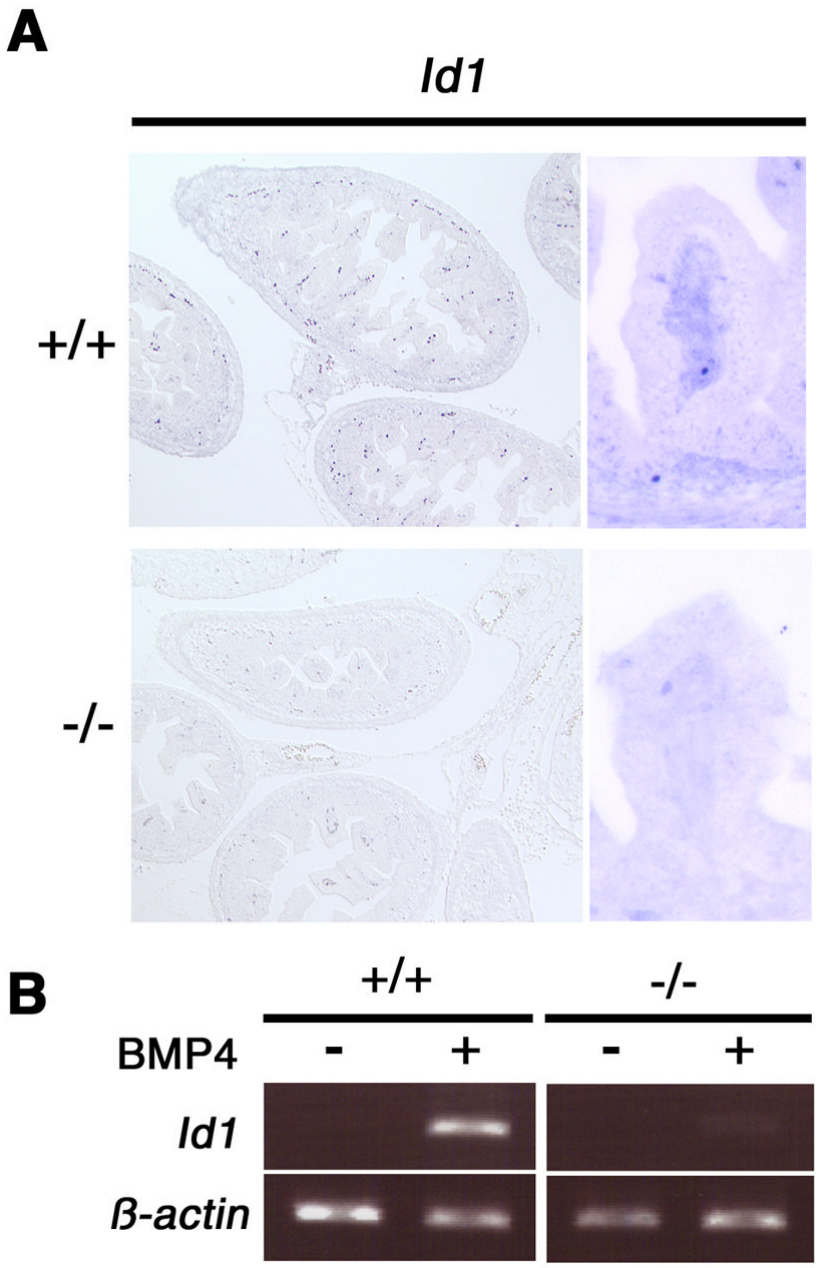

Figure 5. TAB1 is involving in BMP signaling cascade

A. Expression analysis of *Id1* in *Tab1* mutants at E16.5. *Id1* expression levels were downregulated in mesenchymal regions of intestine in *Tab1* mutant embryos.

B. Wild type and *Tab1*-deficient (−/−) MEFs were cultured with BMP4 and *Id1* expression was determined by RT-PCR. An increase in *Id1* expression levels was observed in BMP4-treated control MEFs, however there was no induction of *Id1* expression in *Tab1*-deficient (−/−) MEFs after stimulated by BMP4. β-actin was used as an internal control.